J|A|C|S
ARTICLES
Published on Web 02/21/2004

Substrate Affinities for Membrane Transport Proteins Determined by ^{13}C Cross-Polarization Magic-Angle Spinning Nuclear Magnetic Resonance Spectroscopy

Simon G. Patching,[†] Adrian R. Brough,[‡] Richard B. Herbert,[†] J. Anton Rajakarier,[†] Peter J. F. Henderson,[†] and David A. Middleton*[,§]

Contribution from the Department of Biomolecular Sciences, University of Manchester Institute of Science and Technology, Sackville Street, Post Office Box 88, Manchester M60 1QD, United Kingdom, and Astbury Centre for Structural Molecular Biology and Institute of Materials Research and School of Civil Engineering, University of Leeds, Leeds LS2 9JT, United Kingdom

Received July 9, 2003; E-mail: david.a.middleton@umist.ac.uk

Abstract: We have devised methods in which cross-polarization magic-angle spinning (CP-MAS) solid-state NMR is exploited to measure rigorous parameters for binding of ^{13}C-labeled substrates to membrane transport proteins. The methods were applied to two proteins from *Escherichia coli*: a nucleoside transporter, NupC, and a glucuronide transporter, GusB. A substantial signal for the binding of methyl [1-^{13}C]-β-D-glucuronide to GusB overexpressed in native membranes was achieved with a sample that contained as little as 20 nmol of GusB protein. The data were fitted to yield a K_D value of 4.17 mM for the labeled ligand and 0.42 mM for an unlabeled ligand, *p*-nitrophenyl β-D-glucuronide, which displaced the labeled compound. CP-MAS was also used to measure binding of [1′-^{13}C]uridine to overexpressed NupC. The spectrum of NupC-enriched membranes containing [1′-^{13}C]uridine exhibited a large peak from substrate bound to undefined sites other than the transport site, which obscured the signal from substrate bound to NupC. In a novel application of a cross-polarization/polarization-inversion (CPPI) NMR experiment, the signal from undefined binding was eliminated by use of appropriate inversion pulse lengths. By use of CPPI in a titration experiment, a K_D value of 2.6 mM was determined for uridine bound to NupC. These approaches are broadly applicable to quantifying binding of substrates, inhibitors, drugs, and antibiotics to numerous membrane proteins.

Introduction

The process of drug discovery is assisted by a range of experimental techniques that are used to identify lead compounds with moderate to high affinity for the pharmacological target molecule in vitro. Nuclear magnetic resonance (NMR) spectroscopy has emerged as a valuable tool in drug discovery for detecting the association of small molecules with purified receptors of pharmaceutical interest and for determining their binding constants.[1−5] Most current NMR screening methods involve the detection of spectra of weakly binding ligands in solution and in large excess over the concentration of a soluble protein. These methods exploit various physical properties of the ligand in solution that are modulated by its transitory association with the receptor (e.g., diffusion coefficients,[6] transferred NOEs,[7] or saturation transfer[8]). The choice of NMR method to be used is influenced by issues of throughput rate, size and concentration of the target, affinity of the ligand, and the accuracy and precision of the binding constants obtained.

Over half the targets of current drug therapies are membrane-embedded proteins,[9] which usually must be isolated in a lipid bilayer to preserve their structure and function. Solution NMR has recently been used to detect weak interactions between ligands and membrane-spanning proteins, for example, integrin,[10] but the size, heterogeneity, and insolubility of membranes generally present considerable experimental difficulties. Strongly bound ligands undergoing slow dissociation rates from membrane receptors cannot be detected directly by conventional NMR methods because the resonance lines are broadened by chemical shift anisotropy (CSA) and dipolar interactions within the binding site. Binding constants of ligands undergoing slow exchange between the free and bound states have been

* To whom correspondence should be addressed: Tel +44 161 2004217; fax +44 161 2360409.
[†] Astbury Centre for Structural Molecular Biology, University of Leeds.
[‡] Institute of Materials Research and School of Civil Engineering, University of Leeds.
[§] University of Manchester Institute of Science and Technology.

(1) Hajduk, P. J.; Burns, D. J. *Comb. Chem. High Throughput Screening* **2002**, *5*, 613−621.
(2) Dalvit, C.; Flocco, M.; Knapp, S.; Mostardini, M.; Perego, R.; Stockman, B. J.; Veronesi, M.; Varasi, M. *J. Am. Chem. Soc.* **2002**, *124*, 7702−7709.
(3) Dalvit, C.; Fasolini, M.; Flocco, M.; Knapp, S.; Pevarello, P.; Veronesi, M. *J. Med. Chem.* **2002**, *45*, 2610−2614.
(4) Hajduk, P. J.; Bures, M.; Praestgaard, J.; Fesik, S. W. *J. Med. Chem.* **2000**, *42*, 3443−3447.
(5) Hajduk, P. J.; Gerfin, T.; Böhlen, J.-M.; Häberli, M.; Marek, D.; Fesik, S. W. *J. Med. Chem.* **1999**, *42*, 2315−2317.
(6) Yan, J.; Kline, A. D.; Mo, H.; Zartler, E. R.; Shapiro, M. J. *J. Am. Chem. Soc.* **2002**, *124*, 9984−9985.
(7) Mayer, M.; Meyer, B. *J. Med. Chem.* **2002**, *43*, 2093−2099.
(8) Mayer, M.; Meyer; B. *J. Am. Chem. Soc.* **2001**, *123*, 6108−6127.
(9) Drews, J. *Science* **2000**, *287*, 1960−1964.
(10) Meinecke, R.; Meyer, B. *J. Med. Chem.* **2001**, *44*, 3059−3065.

10.1021/ja037163i CCC: $27.50

determined indirectly via solution NMR by displacing the observed ligand with a competitive ligand,[2] but first it is necessary to determine the K_D of the displacing species by an independent method. Moreover, the requirement for a large excess of ligand over the receptor can promote nonspecific binding of poorly soluble ligands with the hydrophobic interior of the lipid membrane, which can obscure the pharmacologically relevant interactions and introduce substantial errors.

Cross-polarization magic-angle spinning (CP-MAS) is a standard solid-state NMR technique that is also capable of detecting the interactions of ligands with membrane proteins, regardless of size or function, and with binding affinities ranging from nanomolar to over millimolar.[11−13] When a suitably isotopically labeled (e.g., ^{13}C, ^{15}N, or ^{19}F) ligand is added to a membrane sample, the ligand produces an NMR signal only if its motion is restrained by interactions with the membrane protein target. The advantage of the CP-MAS approach is that CSA and dipolar interactions are reduced or eliminated, so that both strongly and weakly binding ligands can be observed equally well without adjustment of the experimental conditions. A further advantage of CP-MAS is that the sample spinning reduces susceptibility to broadening, giving sharper lines and higher signal-to-noise ratios. The potential value of this technique for quantifying ligand affinities for membrane receptors has yet to be demonstrated, however.

In our studies here, variable contact time ^{13}C CP-MAS NMR has been investigated as a novel method for determining the binding affinities of membrane protein ligands. The method was tested on two transport proteins from *Escherichia coli*, GusB and NupC, for which we had achieved 20−50-fold amplification of their expression so they comprised approximately 30% of total protein in inner membrane preparations.[14] Some 5−12% of all proteins are membrane transport proteins,[15] and their roles in antibiotic resistance, toxin secretion, and tumor growth make them important drug targets.[16] The glucuronide−H^+ symport protein GusB[17,18] transports alkyl or aryl β-D-glucuronides, the conjugates by which xenobiotics or drugs are excreted from the human body. Importantly, we had already devised synthetic procedures to make ^{13}C-labeled glucuronide ligands for GusB.[17] GusB is predicted to comprise 12 transmembrane α-helices, typical of numerous membrane transport proteins in all organisms, although it is itself probably unique to bacteria as searches have not so far found homologues in other types of organisms with sequenced genomes. By contrast, the nucleoside−H^+ symport protein NupC is predicted to comprise 10 transmembrane α-helices[19] and is a bacterial homologue of an important mammalian transporter, CNT1, which provides the route for entry of the hormone adenosine and of nucleoside drugs such as AZT into cells.[20]

The binding affinities of two ^{13}C-labeled substrates were examined: the GusB substrate methyl [1-^{13}C]-β-D-glucuronide ([^{13}C]MG) and the NupC substrate [1′-^{13}C]uridine. Substrates of transport proteins generally have low binding affinities (K_D ∼ millimolar) but undergo slow dissociation from the binding site(s) to allow for translocation across the membrane. These overexpressed proteins and their substrates are therefore ideal models of pharmacologically relevant systems on which to test the CP-MAS NMR approach.

Experimental Section

Labeled Compounds. Methyl [1-^{13}C]-β-D-glucuronide was synthesized as follows: [1-^{13}C]-D-Glucose (Cambridge Isotope Laboratories, 99% ^{13}C) (0.5 g, 2.76 mmol) was converted into [1-^{13}C]-1-bromo-2,3,4,6-tetra-*O*-acetyl-α-D-glucose [(i) Ac_2O/pyridine, room temperature (rt) 20 h; (ii) 30% HBr−AcOH/Ac_2O/DCM, rt 18 h; 100%].[21,22] Methyl [1-^{13}C]-2,3,4,6-tetra-*O*-acetyl-β-D-glucoside was prepared from this material (MeOH/Ag_2CO_3–$CaSO_4$, rt 20 h; 72%),[23] and the product was converted into methyl [1-^{13}C]-β-D-glucoside (NaOMe/MeOH, rt 20 h; 100%), which was efficiently oxidized to methyl [1-^{13}C]-β-D-glucuronide (TEMPO, t-BuOCl, H_2O, pH 10−10.5; 100%).[18] δ_H (250 MHz; D_2O) 4.24 (1H, dd, $J_{1,2}$ = 7.9 Hz, $J_{1,C-1}$ = 161.6 Hz, H-1); δ_C (62.9 MHz; D_2O) 176.2 (C=O), 103.5 (C-1, ^{13}C-enriched), 76.1 (C-5), 75.9 (C-3, d, $J_{1,3}$ = 13.0 Hz), 73.2 (C-2, d, $J_{1,2}$ = 46.8 Hz), 72.1 (C-4), 57.8 (O*C*H_3, d, J_{1,CH_3} = 1.8 Hz); *m*/*z* (ES) 208 (100%, M^- − H). [1′-^{13}C]-Uridine (99% ^{13}C) was purchased from Cambridge Isotope Laboratories.

Membrane Preparation. *E. coli* strain NO2947(pWJL24H) containing the plasmid overexpressing the GusB(His)$_6$ protein and strain BL21DE3(pGJL16) overexpressing the NupC protein were grown in 25 L of minimal medium in a fermentor.[14] At the optimal stage of growth established in pilot studies, 0.5 mm isopropyl β-D-thiogalactoside (IPTG) was added to induce expression. Inside-out vesicles were prepared from the genetically engineered organisms by explosive decompression in a French press, and the inner-membrane fraction was isolated by sucrose-density gradient ultracentrifugation.[14] Membrane vesicles were washed three times by suspension in 20 mM Tris-HCl buffer (pH 7.5) followed by ultracentrifugation before final suspension in the same buffer for storage at −80 °C after rapid freezing. Total protein concentration in the vesicle suspension was determined by the method of Schaffner and Weissmann,[24] of which GusB(His)$_6$ or NupC was estimated to comprise between 25% and 35% according to densitometry measurements on the proteins resolved by SDS−PAGE and stained with Coomassie blue. Membranes without GusB(His)$_6$ or NupC overexpression for use as controls were prepared in the same way from cells that contained the plasmid pTTQ18 without the transport gene insert.[14]

Sample Preparation for NMR. The NMR measurements on GusB were performed with membranes that contained between 20 nmol of

(11) Spooner, P. J. R.; Rutherford, N. G.; Watts, A.; Henderson, P. J. F. *Proc. Natl. Acad. Sci. U.S.A.* **1994**, *91*, 3877−3881.
(12) Spooner, P. J. R.; O'Reilly, W. J.; Homans, S. W.; Rutherford, N. G.; Henderson, P. J. F.; Watts, A. *Biophys. J.* **1998**, *75*, 2794−2800.
(13) Middleton, D. A.; Robins, R.; Feng, X.; Levitt, M. H.; Spiers, I. D.; Schwalbe, C.; Reid, D. G.; Watts, A. *FEBS Lett.* **1997**, *410*, 269−274.
(14) Ward, A.; Sanderson, N. M.; O'Reilly, J.; Rutherford, N. G.; Poolman, B.; Henderson, P. J. F. In *Membrane Transport—A Practical Approach*; Baldwin, S. A., Ed.; Oxford University Press: Oxford, U.K., 2000; Chapt. 6, pp 141−166.
(15) (a) Paulsen, I. T.; Sliwinski, M. K.; Saier, M. H. *J. Mol. Biol.* **1998**, *277*, 573−592. (b) Paulsen, I. T.; Nguyen, L.; Sliwinski, M. K.; Rabus, R.; Saier, M. H. *J. Mol. Biol.* **1998**, *301*, 75−101.
(16) (a) van Veen, H. W.; Higgins, C. F.; Konings, W. N. *In Microbial Multidrug Efflux*; Horizon Scientific Press: Wymondham, U.K., 2002; Chapt. 8, pp 99−119. (b) Ouellette, M.; Legare, D.; Papadopolou, B. In *Microbial Multidrug Efflux*; Horizon Scientific Press: Wymondham, U.K., 2002; Chapt. 10, pp 141−154.
(17) (a) Liang, W.-j. Ph.D. Thesis, Cambridge University, U.K., 1992. (b) Poolman, B.; Knol, J.; Van der Does, C.; Henderson, P. J. F.; Liang, W.-j; Leblanc, G.; Pourcher, T.; Mus-Veteau, I. *Mol. Microbiol.* **1996**, *19*, 911−922.
(18) (a) Melvin, F. Ph.D. Thesis, University of Leeds, England, 2000. (b) Melvin, F.; MacNeill, A.; Henderson, P. J. F.; Herbert, R. B. *Tetrahedron Lett.* **1999**, *40*, 1201−1202.
(19) Craig, J. E.; Zhang, Y.; Gallagher, M. P. *Mol. Microbiol.* **1994**, *11*, 1159−1168.
(20) (a) Ritzel, M. W. L.; Yao, S. Y. M.; Huang, M. Y.; Elliot, J. F.; Cass, C. E.; Young, J. D. *Am. J. Physiol.* **1997**, *272*, C707−C714. (b) Ritzel, M. W. L.; Ng, A. M. L.; Yao, S. Y. M.; Graham, K.; Loewen, S. K.; Smith, K. M.; Hyde, R. J.; Karpinski, E.; Cass, C. E.; Baldwin, S. A.; Young, J. D. *Mol. Membr. Biol.* **2001**, *18*, 65−72.
(21) Shimizu, H.; Brown, J. M.; Homans, S. W.; Field, R. A. *Tetrahedron* **1998**, *54*, 9489−9506.
(22) Ohrui, H.; Horiki, H.; Kishi, H.; Meguro, H. *Agric. Biol. Chem.* **1983**, *47*, 1101−1106.
(23) Conchie, J.; Levy, G. A. *Methods Carbohydr. Chem.* **1963**, *2*, 86.
(24) Schaffner, W.; Weissmann, C. *Anal. Biochem.* **1973**, *56*, 502−514.

GusB (5 mg of total protein) and 80 nmol of GusB (20 mg of total protein), depending on the size of the NMR sample rotor (4 or 6 mm external diameter) that was available for the experiments. The membranes were suspended to 2 mL in Tris-HCl buffer (20 mM, pH 7.5) to which the required concentration of [^{13}C]MG was added, with brief vortexing to mix the sample, followed by equilibration at 4 °C for 30 min. The membranes were collected by ultracentrifugation (10000*g*) and then packed into the NMR sample rotor by a brief slow spin in a benchtop centrifuge. Control measurements were performed as above with control membranes that contained the same amount of total protein as used in the GusB membranes. The titration of competitive substrate into GusB membranes to displace [^{13}C]MG binding was performed by making a series of additions directly to the sample in the NMR rotor. A Hamilton syringe was used to make 5−10 μL additions of a 200 mM solution of the competitive substrate in Tris-HCl (20 mM, pH 7.5) to the membranes in the rotor; mixing was achieved by gently stirring the membrane suspension with the needle of the syringe. The sample was then packed to the bottom of the rotor by a very brief, slow, spin in a benchtop centrifuge and then equilibrated at 4 °C for 30 min.

The measurements on NupC were performed with membranes that contained 70 nmol of NupC (15 mg of total protein) or 150 nmol of NupC (32 mg of total protein). Control measurements were performed with membranes that contained the same amount of total protein as used in the NupC membranes but without overexpressed NupC (see above). [1′-^{13}C]Uridine (5 mM) was added to the membranes as described above for the addition of [^{13}C]MG to GusB membranes. The addition of the competing substrate thymidine (50 mM) was performed by resuspending the membranes in the retained supernatant from the ultracentrifuge spin in which 50 mM thymidine had been dissolved. Following equilibration at 4 °C for 30 min, the membranes were collected by ultracentrifugation and then returned back into the sample rotor.

NMR Conditions. Early NMR measurements were performed on a Bruker MSL300 MHz spectrometer. Later experiments were performed on a Varian InfinityPlus 300 operating at a magnetic field of 7 T and a Bruker Avance 400 spectrometer operating at a magnetic field of 9.3 T. The sample temperature was 4 °C in all experiments. Standard ^{13}C CP-MAS experiments were performed with double-tuned probe heads at a sample spinning frequency of 2.4 kHz on the 300 MHz instrument and 4 kHz on the 400 MHz instrument. The diameter of the NMR sample rotor was 6 mm for experiments on the 300 MHz instrument and 4 mm for experiments on the 400 MHz instrument. At 300 MHz, 40 kHz radio frequency was used for all pulses. At 400 MHz following a ^{1}H 90° pulse length of 3.5−4.0 μs, Hartmann−Hahn cross-polarization from ^{1}H to ^{13}C was attained at contact times ranging from 100 μs to 10 ms with matched ^{1}H and ^{13}C fields of 65 kHz. Continuous-wave proton decoupling at a field of 85 kHz was applied during signal acquisition. Experiments to remove signals from nonspecific substrate binding used the pulse sequence for cross-polarization with polarization inversion (CPPI) of Wu and Zilm.[25] Following a contact time of 750 μs, the Hartmann−Hahn condition was maintained but the phase of the ^{1}H transmitter was shifted by 180° and pulses were applied simultaneously at the frequencies of ^{1}H and ^{13}C for a duration (t_{PI}) of 1−60 μs. During this period, the equilibrium state is perturbed and ^{13}C magnetization is transferred back to the proton spins. Finally, continuous-wave proton decoupling at a field of 85 kHz was applied during signal acquisition.

Theory

The ^{13}C CP-MAS NMR experiment generates signals from low-abundance ^{13}C spins by transferring magnetization from abundant ^{1}H spins, which for rigid solids can produce gains in ^{13}C signal intensity and reduce the experimental time. The experiment first excites ^{1}H magnetization and then applies Hartmann−Hahn matched spin-locking fields simultaneously at the resonance frequencies of ^{13}C and ^{1}H for a duration t_c known as the contact time. Magnetization is transferred from ^{1}H to ^{13}C at a rate $1/T_{HC}$ (where T_{HC} is the time constant for cross-polarization) during the contact time, provided the ^{1}H−^{13}C dipolar coupling constants d_{HC} are nonzero, which is generally true for rigid solids. Simultaneously the ^{1}H spins relax at a rate $1/T_{1\rho H}$, where $T_{1\rho H}$ is the spin−lattice relaxation time of ^{1}H in the rotating frame. After the contact period the ^{13}C signal is detected while ^{1}H interactions are removed by high-power decoupling. The signal intensity S after t_c can be approximated as[26]

$$S = S_0\left(1 - \frac{T_{HC}}{T_{1\rho H}}\right)^{-1}\left[\exp\left(-\frac{t}{T_{1\rho H}}\right) - \exp\left(-\frac{t}{T_{HC}}\right)\right] \qquad (1)$$

where S_0 is the theoretical maximum signal intensity attainable.

In our studies here, ^{13}C-labeled substrates were added to aqueous suspensions of membranes containing the target protein and ^{13}C NMR peak intensities were measured for different substrate concentrations over a range of contact times. Curves were fitted to the peak intensity profiles to extract binding constants ($1/K_D$) for the substrates and the rate constants (k_{off}) for their dissociation from the binding site. To understand how binding constants can be determined by CP-MAS, it is necessary to evaluate how the substrate signal intensity is influenced by the trajectories of the molecules as they move in to and out of the binding site during t_c. Consider a substrate molecule that is not bound at the start of the CP-MAS contact time. The ^{1}H−^{13}C dipolar coupling constant for that substrate is averaged to zero by rapid isotropic tumbling of the molecule in solution and the ^{13}C spins remain at equilibrium. If at some point during t_c the substrate binds to a receptor site, d_{HC} becomes nonzero so that the ^{13}C magnetization builds up at a rate $1/T_{HC}$ because the magnetization is now able to transfer from the ^{1}H spins to the ^{13}C spins. The transfer process is damped by ^{1}H and ^{13}C relaxation in the rotating frame with rates $1/T_{1\rho H}^{bound}$ and $1/T_{1\rho C}^{bound}$. The substrate remains bound to the receptor for a residency time t_{on}, after which it reverts to the free state. The ^{13}C magnetization accrued up to this point relaxes back toward equilibrium at rates $1/T_{1\rho H}^{free}$ and $1/T_{1\rho C}^{free}$ and no further transfer occurs unless the substrate binds to the receptor again. The magnetization remaining at the beginning of the acquisition period is observed as the free induction decay.

Substrate exchange in and out of the receptor site can occur many times during t_c depending on its affinity for the protein and the concentration of available binding sites. The evolution of ^{13}C magnetization M_C for an ensemble of N ligands undergoing exchange between free and bound environments can be expressed by

$$M_C(t_c) = \sum_N\left[\int_0^{t_1}\frac{dm_C^{\,1}}{dt} + \int_{t_1}^{t_2}\frac{dm_C^{\,2}}{dt} + \int_{t_2}^{t_3}\frac{dm_C^{\,1}}{dt} \ldots\right] \qquad (2)$$

where m_C represents the magnetization from individual ligand molecules at time t during the contact period. The indices 1 and 2 refer to the free and bound states of the ligand, in either order, and t_i and t_{i+1} are the times during t_c at which the ligand joins and leaves each of the two states. The differential terms in eq 2 can be adapted from standard equations[27] to obtain expanded expressions for the bound ligand:

$$\frac{dm_C^{\,bound}}{dt} = -(m_C - m_H)/T_{HC}^{\,bound} - m_C/T_{1\rho C}^{\,bound} \qquad (3a)$$

$$\frac{dm_H^{\,bound}}{dt} = -k(m_H - m_C)/T_{HC}^{\,bound} - m_H/T_{1\rho H}^{\,bound} \qquad (3b)$$

When the ligand is in the free state, the terms containing T_{HC} become

(25) Wu, X.; Zilm, K. W. *J. Magn. Reson.* **1993**, *102*, 205−213.

(26) Stejskal, E. O.; Memory, J. D. *High-Resolution NMR in the Solid State*; Oxford University Press: Oxford, U.K., 1994.

(27) Kolodziejski, W.; Klinowski, J. *Chem. Rev.* **2002**, *102*, 613−628.

zero and the equations simplify to

$$\frac{dm_C^{free}}{dt} = -m_C/T_{1\rho C}^{free} \quad (3c)$$

$$\frac{dm_H^{free}}{dt} = -m_H/T_{1\rho H}^{free} \quad (3d)$$

where k is a scaling factor. Hence, the ^{13}C signal intensity for the substrate is modulated by its residency time t_{on} in the binding site and by the frequency of binding episodes during the contact time, which is a function of K_D.

Here, the binding trajectories of individual substrate molecules over contact periods of up to 10 ms were simulated by a general Monte Carlo approach, in which the substrate binding episodes were determined by a probability factor. First, the initial state, free or bound, of a single molecule when $t_c = 0$ was determined randomly, weighted by the probability of a ligand occupying a vacant receptor site (F_b), defined as

$$F_b = \frac{[RL]_{eq}}{[L]_T} = \frac{1}{2[L]_T}\{K_D + [L]_T + [R]_T - \sqrt{(K_D + [L]_T + [R]_T)^2 - 4[L]_T[R]_T}\} \quad (4)$$

where $[RL]_{eq}$ is the equilibrium concentration of the complex and $[L]_T$ and $[R]_T$ are the total concentrations of ligand and receptor. Hence, as K_D increases, F_b decreases and the probability of ligand binding is reduced. The dissociation of the substrate from the receptor is a first-order process and the residency time of a substrate in its binding site was determined randomly, weighted by a probability factor F_d defined as

$$F_d = \exp(-k_{off}t_b) \quad (5)$$

where t_b is the length of time spent in the binding site and k_{off} is the dissociation rate constant. When the ligand has left the binding site, further episodes of binding to a free receptor were again determined randomly according to F_b. By combination of the Monte Carlo approach with eqs 2 and 3, it was possible to calculate the relationship between K_D and the CP-MAS signal intensity for an ensemble of N substrate molecules. The total signal after t_c could be calculated for any pair of K_D and k_{off} values by substituting the known or estimated values of the $T_{1\rho}$ relaxation times for ^1H and ^{13}C, the rate of magnetization transfer ($1/T_{HC}$), and the concentrations of ligand [L] and protein [P].

Simulated profiles of signal intensity as a function of t_c for a hypothetical ligand (6 mM) bound to a membrane receptor (1.6−2.4 mM) are shown in Figure 1. The simulations illustrate how the shape of the intensity profile is modulated if K_D is kept constant and k_{off} is increased (i.e., the residency time is shortened). As k_{off} increases, the signal intensity profiles reach their maxima at progressively longer contact times because the overall rate of magnetization transfer is lowered as the ligand spends more time in the free state. Further, the maximum attainable signal intensity increases because greater numbers of molecules undergo magnetization transfer in the bound state over short periods before relaxation processes become dominant. If K_D is increased but k_{off} is kept constant, both the rate of magnetization transfer and the maximum signal intensity are lowered because the probability of binding F_b is reduced (Figure 1). The simulations show, therefore, that the shape of the intensity profile is highly dependent on K_D and k_{off}. The simulations also indicate that the peak intensity curves for protein concentrations of 1.6 mM (dotted line), 2.0 mM (solid line), and 2.4 mM (dashed line) are very similar to each other. The variance is highest for low-affinity, weakly binding ligands (e.g., $K_D = 10$ mM, $k_{off} = 1000\ s^{-1}$) at long contact times. Hence, it is expected that a 20% error in the measured protein concentration will have little effect on the observed peak intensities and on the calculated value of K_D.

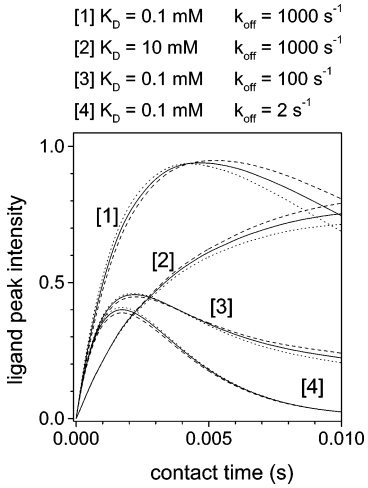

Figure 1. Simulations of CP intensity profiles for a ligand interacting with a membrane protein, calculated for different values of the dissociation rate constant (k_{off}) and the dissociation constant (K_D) as shown (1−4). Simulations were carried out according to the procedure described in the Theory section, with constant values for the ligand concentration (6 mM), T_{HC} (1.5 ms), $T_{1\rho H}^{free}$ (100 ms), and $T_{1\rho H}^{bound}$ (2 ms). The simulations represent protein concentrations of 2.4 mM (dashed line), 2.0 mM (solid line) and 1.6 mM (dotted line). In all simulations it was assumed that the relaxation rates for ^{13}C are long compared to the contact time.

The simulations in Figure 1 show that, in propitious circumstances, specific values of K_D and k_{off} can be extracted directly from an experimental peak intensity profile obtained for a single ligand concentration. It will be shown, however, that when nonspecifically bound substrate contributes to the NMR peak intensities, K_D must be determined in a titration experiment in which peak intensities are measured for a range of substrate concentrations.

Results and Discussion

Binding of a ^{13}C-Labeled Glucuronide to GusB. In Figure 2 are shown the ^{13}C CP-MAS spectra of *E. coli* membrane samples containing 80 nmol of GusB and the substrate [^{13}C]-MG. The spectrum of membranes containing [^{13}C]MG at a concentration of 6 mM exhibited a signature peak from the substrate at 103 ppm (Figure 2A); the substrate must interact with the membrane in order for $^1H-^{13}C$ magnetization transfer to occur and for the signal to be detected. The dominant mechanism for magnetization transfer is the residual dipolar interaction between ^1H and ^{13}C ($d_{HC} < 10\,000$ Hz), which is present only when the substrate is bound to the membranes. Other mechanisms for transfer, such as scalar coupling, which is not motionally averaged, were expected to be insignificant under the conditions of the CP-MAS experiments described here. This was confirmed by conducting CP-MAS NMR experiments on 20 mM [^{13}C]MG in aqueous solution. No signal from the labeled substrate was obtained after 10 000 scans when contact times of up to 10 ms were used (data not shown). An SDS−polyacrylamide gel of the membranes (Figure 2, top right) confirmed that GusB overexpression was induced and that the level of expression was about 25% of total membrane protein. The experiment required 3 h of signal acquisition to attain the substrate peak intensity shown in Figure 2A. To test the limits of detection of the CP-MAS application, a spectrum was obtained from a fresh membrane sample containing 20 nmol of GusB and 20 mM [^{13}C]MG (Figure 2B). The peak intensity at

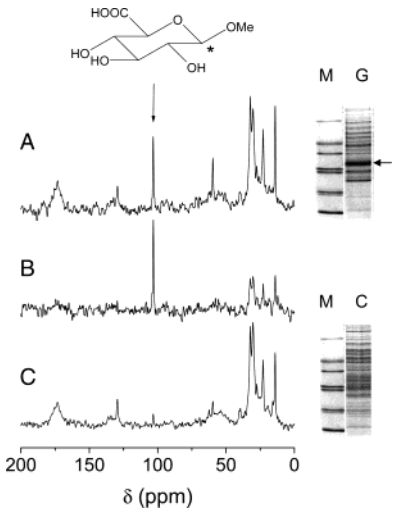

Figure 2. Representative ^{13}C CP-MAS NMR spectra of *E. coli* membrane samples containing the labeled substrate [^{13}C]MG. Spectra were acquired by accumulating 10 240 transients (~3 h acquisition time) from a membrane sample containing 80 nmol of GusB (100 μL sample volume) and 6 mM substrate (A) or 1024 transients (~18 min acquisition time) from 20 nmol of GusB (25 μL sample volume) and 20 mM substrate (B). The vertical arrow denotes the peak at 103 ppm from the labeled substrate. An SDS−polyacrylamide gel of GusB-enriched membranes (lane G) and marker proteins (lane M) is shown to the right of the spectra, with the band for GusB indicated by the horizontal arrow. The molecular masses of the markers were 66, 45, 36, 29, 24, 20.1, and 14.2 kDa. A spectrum was also acquired (10 240 scans) from control *E. coli* membranes, i.e., without GusB, containing 6 mM [^{13}C]MG (C). An SDS−polyacrylamide gel of control membranes (lane C) is shown to the right of the spectrum. Spectra were recorded with a spinning rate of 4.028 kHz, a 10-ms contact time, a 1-s recycle delay, and a temperature of 4 °C. The chemical structure of the substrate is shown at the top, and the position of the ^{13}C label is denoted by an asterisk.

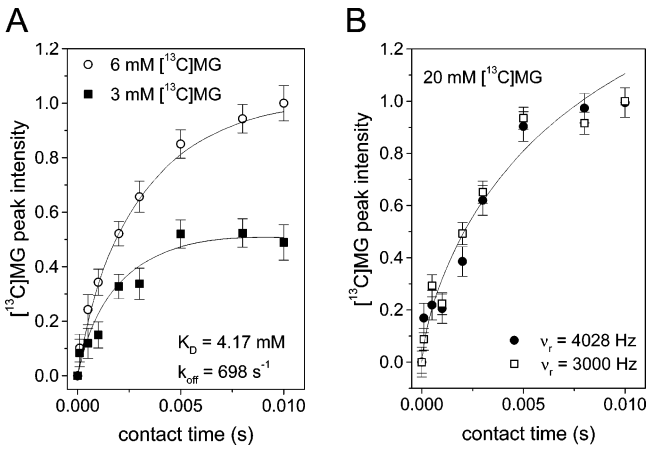

Figure 3. Experimental and simulated ^{13}C CP-MAS NMR intensity profiles for [^{13}C]MG in GusB-enriched membranes. Substrate peak intensities at 103 ppm were measured from spectra of *E. coli* membranes containing GusB (80 nmol; 100 μL sample volume) and [^{13}C]MG at a concentration of 3 mM (■) or 6 mM (○) and are plotted against contact time t_c (A). The best-fitting simulations of intensity profiles (solid lines) correspond to the values of K_D and k_{off} shown. Simulations were carried out for T_{HC} = 0.2 ms, $T_{1\rho H}^{free}$ = 100 ms, and $T_{1\rho H}^{bound}$ = 3.5 ms. Other simulation parameters were as described for Figures 2 and 3. Also shown are substrate peak intensities measured from a different batch of *E. coli* membranes containing 20 nmol of GusB and 20 mM [^{13}C]MG spinning at MAS frequencies (ν_r) of 4028 and 3000 Hz (B). The simulated intensity profile (solid line) was calculated with the parameters described for panel A but substituting the new concentrations of protein and substrate.

103 ppm was comparable to that attained at the higher GusB concentration after less than 20 min of acquisition time. The gain in sensitivity occurs because the substrate undergoes fast rates of dissociation from the binding site (Figure 1) and the high [^{13}C]MG concentration (20 mM) enables more substrate molecules to experience cross-polarization during the contact time than at the lower substrate concentration. Such gains in sensitivity would not be made in the case of slowly dissociating substrates. A spectrum of 6 mM [^{13}C]MG added to control membranes from *E. coli* in which GusB expression was not induced (Figure 2C) exhibited only a minor peak at 103 ppm, which probably represented nonspecifically bound substrate and which was approximately 5% of the peak intensity in GusB membranes. The control experiment confirmed that, in the GusB spectrum, the contribution from nonspecific binding to the substrate signal was very small and that the signal represented, predominantly, substrate bound to the transport protein.

Peak intensities over contact times from 100 μs to 10 ms were measured from the spectra of membranes containing 80 nmol of GusB and two different concentrations of [^{13}C]MG (Figure 3A). Values of k_{off} and K_D were determined from a two-parameter fit of simulated curves to the experimental data for the two substrate concentrations (3 and 6 mM). Although in favorable cases a unique combination of K_D and k_{off} values can be obtained from a single intensity profile, here two profiles for different substrate concentrations were collected to be certain of removing any ambiguities in the calculated values. Curve-fitting was carried out by computing peak intensity profiles for the two substrate concentrations at varying K_D and k_{off} values to minimize the χ^2 function:

$$\chi^2 = \sum_i \left(\frac{S_i - E_i}{\sigma_i} \right)^2 \qquad (6)$$

for the combined sets of data, where E_i is the experimental data point, S_i is the simulated data point, and σ_i is the level of the noise. In the simulations, input values of $T_{1\rho}$ for the free substrates were determined experimentally from relaxation measurements on aqueous ligand solutions. Values of $T_{1\rho}$ and T_{HC} for the bound substrates could not be determined directly, but valid approximations were obtained from the mean $T_{1\rho}$ and T_{HC} values for protonated membrane lipid and protein carbons that are expected to have similar motional characteristics to the bound substrates. Measurements of CP-MAS intensity profiles in the olefinic (125 ppm), aliphatic (25−35 ppm), and protein C_α (50−70 ppm) regions of *E. coli* membrane spectra yielded values of $T_{1\rho H}$ = 3.5 (± 1.0) ms and T_{HC} = 0.2 (± 0.05) ms. Errors may be introduced into the simulations from inaccuracies in the estimates of $T_{1\rho}$ and T_{HC} for the bound substrate, but such errors will be minimal because the range of realistic $T_{1\rho}$ and T_{HC} values is small.

A two-parameter fit to the experimental data for the different substrate concentrations yielded K_D and k_{off} values of 4.17 mM and 698 s^{-1} at the χ^2 minimum (Figure 3A). The simulations yielded a range of simulated curves that fell within the error limits of the experimental data, however. The curves corresponded to values of K_D from 2.53 to 5.68 mM and values of k_{off} from 512 to 817 s^{-1}, which represent the confidence limits of the measurements. The value of K_D is higher than the K_m for energized transport (25−250 μM, depending on the glucuronide used; methyl β-D-glucuronide is toward the top of this range) but is consistent with expectations for unenergized binding of ligand to transport proteins.[12,28]

To test the reproducibility and reliability of the CP-MAS profiles for determining K_D and k_{off}, a further variable contact time CP-MAS experiment was conducted on a separate batch of *E. coli* membranes containing different concentrations of GusB and [^{13}C]MG. In Figure 3B are shown the peak intensities for 20 mM [^{13}C]MG in membranes containing 20 nmol of GusB at different contact times. Also shown is a simulated intensity curve calculated from the same parameters as described for Figure 3A but with the new concentrations of protein and substrate substituted into the calculation. The calculated curve fits closely to the experimental data even without minimization of the χ^2 function, providing good evidence that the CP-MAS is reproducible from sample to sample.

To eliminate the possibility that the sample rotation frequency might influence the intensity build-up curves, the peak intensities in Figure 3B were measured at the two MAS frequencies (ν_r) of 4028 and 3000 Hz. The experiment confirmed that significant differences in the peak intensities did not occur at the two spinning frequencies. In routine applications, the practical range of spinning frequencies is expected fall within the 3000−4000 Hz range, which is sufficiently high to remove the desired interactions but not high enough for the centrifugal force to physically disrupt the sample.

Binding Constants for Unlabeled Substrates. The experiments on [^{13}C]MG confirm that it is possible to determine the binding affinities and dissociation rates of labeled substrates of membrane proteins. The usefulness of this method for determining binding affinities of many different substrates would be limited if isotope labeling were required for each substrate. Therefore, we further investigated whether the observation of [^{13}C]MG binding could be exploited to determine indirectly the K_D value for a nonlabeled, competitive substrate of GusB. It is expected that the peak from [^{13}C]MG in the ^{13}C CP-MAS NMR spectrum will diminish if a competitive substrate reduces the equilibrium concentration of bound [^{13}C]MG. In the Monte Carlo simulations, the probability F_b of labeled ligand binding in the presence of a competing ligand can be estimated according to

$$[RL^*]_{eq} = \frac{[R]_T[L^*]_{eq}/K^*}{(1 + [L^*]_{eq}/K^* + [L]_{eq}/K)} \qquad (7)$$

where $[R]_T$ is the total receptor concentration and [L*] and [L] and K^* and K are the equilibrium concentrations and dissociation constants of labeled and unlabeled ligands, respectively.

A series of spectra was obtained for *E. coli* membranes containing GusB (20 nmol) and 20 mM [^{13}C]MG in the presence of varying concentrations of the unlabeled competitive substrate *p*-nitrophenyl-β-D-glucuronide (NPG).[17,18] The spectra were recorded at a single contact time of 10 ms, which was shown to provide high signal intensity from the labeled ligand at the concentration used (Figure 2). As expected, the peak intensity from the labeled substrate diminished as the concentration of NPG was raised from 0 to 80 mM (Figure 4). By using a low GusB concentration and high [^{13}C]MG concentration, the full series of NMR experiments was completed in 1.5 h. Curve-fitting to the experimental data was performed via the Monte Carlo approach, by substituting into eq 6 the values of K_D and k_{off} determined for [^{13}C]MG in the absence of a competitor substrate (Figure 3) and varying the value of K_D for NPG until the χ^2 function was minimized. The simulation procedure was simplified by replacing the total substrate concentrations (i.e., $[L^*]_T$ and $[L]_T$) in eq 6 with their equilibrium concentrations ([L*] and [L]). This approximation was valid because the molar ratio of GusB to substrate was low (<1:40) and therefore ligand depletion by binding to the transport protein was negligible. When the best-fit value of K_D for [^{13}C]MG (4.17 mM) was substituted into eq 7, the χ^2 function was minimized at a K_D value of 220 μM for NPG (Figure 4). However, when the fact is taken into account that a range of K_D values was obtained for [^{13}C]MG (2.53−5.68 mM), the corresponding K_D values for NPG ranged from 0.13 to 0.39 mM. Hence, in this case the competitive unlabeled substrate has an approximately 10-fold higher affinity for GusB than has [^{13}C]MG.

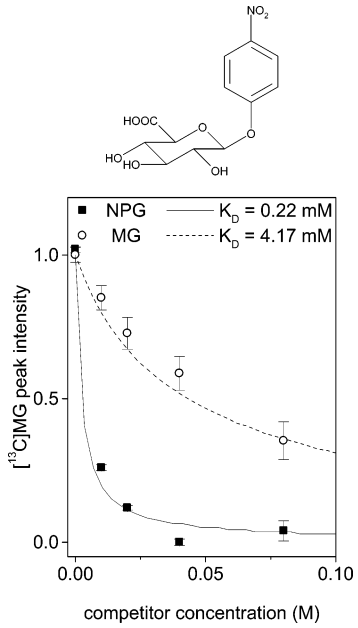

Figure 4. Experimental and simulated ^{13}C CP-MAS intensity curves corresponding to the displacement of [^{13}C]MG from GusB by the unlabeled competitive substrate NPG (shown at the top) and by unlabeled methyl-glucuronide (MG). The displacement of [^{13}C]MG was monitored from the [^{13}C]MG peak intensities at a contact time t_c of 10 ms in the presence of NPG (■) or MG (○) in the concentration range 10−80 mM. Predicted [^{13}C]-MG peak intensities for a range of NPG concentrations were calculated by the Monte Carlo method described in the Theory section, taking into account the expected reduction in the equilibrium concentration ($[RL^*]_{eq}$) of bound [^{13}C]MG for a given competitor K_D value according to eq 7. The simulated curves were based on the K_D value of 4.17 mM for MG determined in Figure 3. The dotted line represents the curve predicted for self-displacement of [^{13}C]MG by unlabeled MG. For the data showing displacement of [^{13}C]-MG by NPG, the best-fitting simulated curve corresponds to a K_D value for NPG of 0.22 mM (solid line). The experiments were conducted on membranes containing 20 nmol of GusB (25 μL sample volume) and 20 mM [^{13}C]MG under conditions as described for Figure 2. The number of scans for each data point was 1024 for displacement by NPG and 512 for displacement by MG.

To assess the accuracy of the dissociation constant when determined by displacement, the experiment was repeated with unlabeled methyl glucuronide as the displacing ligand. If the NMR method is valid, the value of K_D derived for unlabeled MG in competition with [^{13}C]MG should be identical to K_D determined for the labeled substrate by the direct method (Figure

(28) (a) Viitanen, P.; Newman, M. J.; Foster, D. L.; Wilson, T. H.; Kaback, H. R. *Methods Enzymol.* **1986**, *125*, 429−452. (b) Walmsley, A. R.; Petro, K. R.; Henderson, P. J. F. *Eur. J. Biochem.* **1993**, *215*, 43−54. (c) Walmsley, A. R.; Martin, G. E. M.; Henderson, P. J. F. *J. Biol. Chem.* **1994**, *269*, 17009−17019.

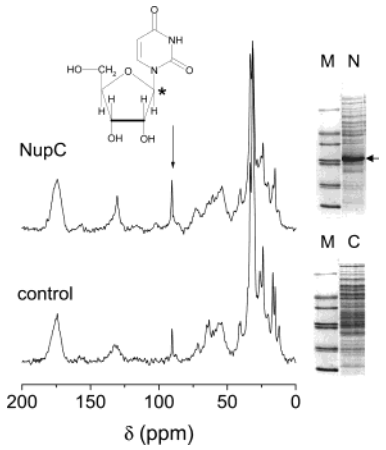

Figure 5. Spectra of the NupC substrate [1-^{13}C]uridine in *E. coli* membranes. Spectra were obtained from membranes containing 150 nmol of NupC in a sample volume of 100 μL (top) and from a control membrane sample purified from bacteria in which the expression of NupC was not induced (bottom). The [1-^{13}C]uridine concentration was 5 mM in both experiments. The vertical arrow denotes the position of the peak from the labeled substrate at 93 ppm. SDS−polyacrylamide gels of NupC-enriched membranes (lane N), control membranes (lane C), and marker proteins (lane M) are shown to the right of the spectra, with the band for NupC indicated by the horizontal arrow. The molecular weight markers are as described for Figure 2. The chemical structure of uridine is shown at the top and the position of the ^{13}C label is denoted by an asterisk. Spectra were recorded at a sample temperature of 4 °C with a spinning rate of 4.028 kHz, a 2-ms contact time, a 1-s recycle delay, and 10 240 scans.

3). In Figure 4 are shown the intensities for [^{13}C]MG in the presence of different concentrations of unlabeled MG (○). The predicted intensity curve for the displacement of [^{13}C]MG, based on the K_D value for MG of 4.17 mM, is also shown in Figure 4 (dotted line). The predicted curve is in excellent agreement with the experimental values. Hence the self-consistency of the displacement experiment further supports the accuracy of the NMR method. It should be noted here that the shape of the NMR displacement curves differs from that of classical competition curves obtained by standard methods such as radioligand binding. This is because, in the situation of fast ligand exchange, the linear relationship between measured peak intensities and the concentration of bound ligand does not hold.

Binding of ^{13}C-Labeled Uridine to NupC. The results for GusB and [^{13}C]MG show that CP-MAS experiments on ligand−receptor interactions are the most time-efficient when the ligand exchanges rapidly between the free and bound states and its concentration is in large excess with respect to the receptor. In many cases, high ligand concentrations may promote nonspecific binding of the ligand to other protein sites or within the lipid bilayer, which will contribute to the observed peak intensity for the ligand. In the case of polar ligands such as [^{13}C]MG, the effect of nonspecific binding on the NMR spectrum is minimal, as confirmed in experiments on GusB-free membranes, which showed no signal from bound [^{13}C]MG. However, hydrophobic ligands have a higher propensity to penetrate into the membrane and in such cases the observed peak intensity in the CP-MAS NMR spectrum may represent both specifically and nonspecifically bound molecules.

Uridine is a substrate for the *E. coli* nucleoside transporter NupC and possesses both polar and hydrophobic characteristics. The ^{13}C spectra of *E. coli* membranes in the presence of [1′-^{13}C]uridine are shown in Figure 5. The spectrum of membranes containing NupC at a concentration of 150 nmol exhibited a peak from the substrate at 92 ppm, well away from the natural-abundance background signal from the membrane proteins and lipids (Figure 5, top). The spectrum of control membranes containing the same concentration of protein and [1′-^{13}C]uridine, but no NupC, also showed a peak at 92 ppm (Figure 5, bottom). Comparison of the two spectra, which were obtained under identical conditions, suggested that approximately 50% of the [1′-^{13}C]uridine peak intensity in the spectrum of NupC membranes was attributable to binding of the substrate to undefined sites other than within NupC. It is essential that this component of the spectrum be removed before the K_D for uridine can be calculated.

Removal of the Undefined Component of the Uridine Signal. Ostensibly, the simplest method for removing the effects of substrate bound to undefined sites is by using difference spectroscopy. An intensity profile for specific binding alone can, in principle, be obtained by subtracting the spectra for control membranes containing [1′-^{13}C]uridine from the spectra of NupC membranes corresponding to total substrate binding. A reliable subtraction can only be achieved if the spectra are obtained from identical concentrations of substrate in control and NupC membranes. This is difficult to achieve in practice because material can be lost when the membrane pellet is transferred to the MAS sample rotor.

An alternative approach was investigated, which exploited the cross-polarization with polarization inversion (CPPI) experiment described by Wu and Zilm.[25] In the CPPI experiment, the phases of the radio frequency pulses are inverted for a short duration t_{PI} after the contact time so that ^{13}C magnetization is transferred back to the ^{1}H spins. The observed ^{13}C signal intensity decreases as the length of t_{PI} is increased, and it passes through zero and becomes negative until eventually thermal equilibrium is reached. At the Hartmann−Hahn condition, the rate of the signal decrease is dependent on the magnitude of the ^{1}H dipolar field experienced by the ^{13}C spins. In its original application, CPPI was used as a spectral editing technique to distinguish between CH_3, CH_2, CH, and nonprotonated carbon signals in ^{13}C spectra of solid materials. The rates of polarization inversion for the different carbon sites are influenced by the effective proton fields and generally follow the order CH_2 > CH > CH_3 > nonprotonated carbon.[25]

Here, the CPPI method was used to observe the single labeled CH site of [1′-^{13}C]uridine, but aimed to distinguish between the substrate molecules in the different binding sites, specific and undefined. It is predicted that the rates and amplitudes of the anisotropic motions experienced by the substrate in the NupC binding site would be different from its motional properties in undefined sites. Differences in motional characteristics will scale to different extents the proton field experienced by the labeled carbon site, which in turn will affect the rates of signal decay in the CPPI experiment. Hence, the CPPI inversion pulse length t_{PI} at which the signal from substrate bound to undefined sites becomes zero is predicted to be different from the pulse length at which the signal from specifically bound signal is eliminated. The advantage of this approach is that the signal from substrate bound to undefined sites can be eliminated selectively according to the motional characteristics of the substrate, and the method is independent of sample concentration. The conditions required for eliminating the signal for ligand bound to sites other than at the specific receptor site may be established in a single

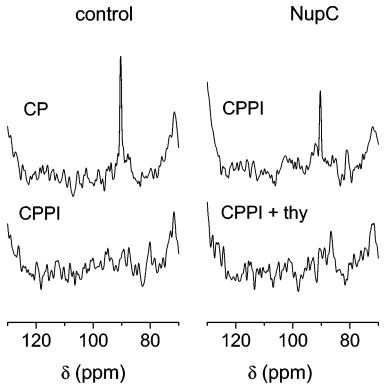

Figure 6. Experimental strategy to eliminate the effects of nonspecific binding of substrate from ^{13}C CP-MAS NMR spectra of [1-^{13}C]uridine in *E. coli* membranes. A ^{13}C CP-MAS spectrum of control membranes containing 5 mM [^{13}C]uridine shows a peak at 92 ppm from nonspecifically bound substrate (top left). A CPPI spectrum with a contact time (t_c) of 750 μs and an inversion pulse length (t_{PI}) of 37 μs eliminates the peak at 92 ppm (bottom left). A CPPI spectrum obtained under identical conditions for membranes (100 μL sample volume) containing 150 nmol of NupC and 5 mM [1-^{13}C]uridine shows a peak from the substrate (top right) that was abolished in the presence of 50 mM thymidine (bottom right). All other conditions were as described for Figure 2.

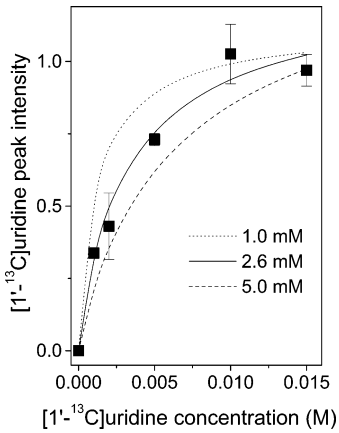

Figure 7. Binding curve for [1-^{13}C]uridine in NupC-enriched *E. coli* membranes obtained by the ^{13}C CPPI experiment. Peak intensities for [1-^{13}C]-uridine were measured after titration of the substrate into membranes (100 μL sample volume) containing 150 nmol of NupC. CPPI spectra were recorded at a contact time (t_c) of 750 μs and an inversion pulse length (t_{PI}) of 37 μs. Simulated binding curves were generated by use of eq 8 for K_D values of 1.0 mM (dotted line), 5.0 mM (dashed line), and 2.6 mM (solid line), which gave the best fit to the experimental data.

calibration experiment and then applied at each substrate concentration during the titration.

In the following, an experimental strategy for eliminating the undefined bound substrate component from CP-MAS spectra of NupC membranes will be described. The results of the experiments are shown in Figure 6. First, a standard ^{13}C CP-MAS NMR spectrum of 5 mM [1′-^{13}C]uridine in control membranes was obtained at a contact time t_c of 750 μs, and the spectrum confirmed that substrate bound to undefined sites could be observed at this contact time (Figure 6, top left). Next, a series of CPPI spectra was obtained from the same sample with a t_c of 750 μs and different values of inversion pulse t_{PI} from 1 to 60 μs, until a pulse length was found (37 μs) at which the substrate peak intensity had decreased to zero (Figure 6, bottom left). The optimized CPPI experiment was then repeated under identical conditions (t_c = 750 μs, t_{PI} = 37 μs) on a sample of NupC membranes containing the same concentration of [1′-^{13}C]-uridine (5 mM). The spectrum for NupC membranes exhibited a peak at 92 ppm from bound substrate, which was absent from the control membranes (Figure 6, top right). The peak could be assumed to represent only specifically bound substrate provided the component from undefined binding had been negated. To confirm that no signal remained from substrate bound to undefined sites, the CPPI experiment was repeated on the sample after addition of the competitive, nonlabeled substrate thymidine to a sufficient concentration (50 mM) to displace [1′-^{13}C]uridine from the NupC binding site, leaving only the nonspecifically bound labeled substrate. The peak from [1′-^{13}C]uridine was fully abolished after addition of thymidine, confirming that the [^{13}C]-uridine signal in the CPPI spectrum was purely from specifically bound substrate and that the component from undefined binding had been successfully removed by polarization inversion (Figure 6, bottom right).

These experiments demonstrate that CPPI is a useful method that exploits differences in motional properties to observe selectively signals from substrates bound to transport proteins and to eliminate signals from substrates bound to undefined sites. Surprisingly, these experiments have revealed that the rate of polarization inversion for nonspecifically bound [1′-^{13}C]uridine is faster than for the substrate bound to NupC. This observation suggests that the rates and amplitudes of motion, which scale the proton dipolar field around the ^{13}C labeled site, are greater for the specifically bound substrate. It might be expected that the binding site within NupC would constrain the substrate more than would nonspecific interactions, but the higher mobility in the NupC site perhaps indicates that nucleoside transport requires only loose associations between substrate and protein.

Determination of the Binding Affinity for Uridine. A titration experiment was performed to determine K_D for uridine, in which the CPPI conditions determined above (t_c = 750 μs, t_{PI} = 37 μs) were applied to eliminate the signal from undefined binding at each substrate concentration. In Figure 7 is shown a plot of peak intensity I for [1′-^{13}C]uridine in NupC membranes as a function of total substrate concentration. The peak intensity reached a maximum value at 10 mM [1′-^{13}C]uridine, indicating that concentration of the substrate was sufficient to saturate the available binding sites. The K_D for uridine was determined by curve fitting to the binding data by use of

$$I([L]_T) = 0.5\{K_D + [L]_T + I_{max} - \sqrt{(K_D - [L]_T - I_{max})^2 - 4[L]I_{max}}\} \quad (8)$$

where I_{max} is the maximum signal intensity attainable at saturating substrate concentrations. The experimental data points lay within curves simulated for K_D values of 1.0 and 5.0 mM, and the best-fitting curve was obtained for a K_D value of 2.6 mM (Figure 7).

Conclusions

NMR-based ligand screening techniques are valuable tools in drug discovery but are underdeveloped for membrane protein targets. Membrane transport proteins comprise 5−15% of genomes in all organisms, from microbe to man.[15] Some classes such as GusB are restricted to bacteria, and so are important in considering specific targets for the development of new antibacterials, e.g., by inhibition of antibiotic efflux proteins.

Others, like NupC, are conserved throughout evolution and are important routes for uptake of drugs into mammalian cells. Such proteins are usually difficult to study because of the need to isolate them in the presence of detergents and to maintain integrity during purification procedures. This work has demonstrated that CP-MAS NMR is an important addition to drug discovery techniques because of its ability to measure binding constants for membrane protein ligands at equilibrium without restrictions on size, exchange rates, or affinity. This is particularly important for membrane transport proteins, where ligand binding affinities can be in the millimolar range, much higher than apparent K_m values. Solid-state NMR also has the important advantage that it utilizes membrane preparations in which the target protein is overexpressed without the need for purification.

A potential limitation of the CP-MAS method is the requirement for appropriately labeled ligands. Some ^{13}C ligands are available commercially, such as [1′-^{13}C]uridine, but others need to be synthesized, as we have done for [^{13}C]MG and uridine labeled at other sites.[30] Alternatively, many pharmacologically active compounds contain ^{19}F, which is a sensitive NMR nucleus with a 100% natural abundance. We are currently investigating the use of ^{19}F CP-MAS for determining affinity constants.[31] The work described here has shown that once one labeled ligand has been obtained, it is possible to determine the binding affinities of many unlabeled ligands indirectly by displacement experiments. Moreover, complementary labeling of targeted residues in the protein may enable the transfer of magnetization between the protein and the bound ligand, leading to elucidation of structural features of the ligand binding sites and the relationship to its binding affinity.

The techniques developed here are particularly important when the ligand is hydrophobic and partitions nonspecifically into a biological membrane as well as binding specifically to a protein target. Many useful drugs are hydrophobic and the ability to discriminate between specific and nonspecific binding is of potential value for numerous compounds and membrane proteins. We already have some 28 bacterial membrane proteins in quantities sufficient for NMR ligand binding studies,[14,29] and there is a wealth of further membrane proteins of biomedical interest to be studied following the sequencing of genomes of organisms from microbes through fungi, parasitic protozoans, plants, and mammals to man. The feasibility of the measurements herein demonstrated for the first time, and their use in determining dissociation constants, especially for weak-binding ligands, augurs wide applicability in the future.

Acknowledgment. We thank BBSRC for support of research in the laboratories of P.J.F.H., D.A.M., and R.B.H.. The work was also sponsored by BBSRC as part of the North of England Structural Biology Centre (NESBiC). S.G.P. acknowledges a postgraduate studentship from EPSRC, and A.R.B., R.B.H., and P.J.F.H. thank EPSRC for an equipment grant GR/R07073/01 to support solid-state NMR at Leeds University. D.A.M. acknowledges the University of Manchester Institute of Technology (UMIST) and BBSRC for funding the NMR facility. Work on NupC is additionally supported by MRC. A.R.B. acknowledges a Leeds University Research Fellowship held in the Schools of Materials and Civil Engineering. We are particularly grateful to John O'Reilly for culturing bacterial strains in a fermentor and for preparations of samples of inner membranes.

JA037163I

(29) (a) Henderson, P. J. F.; Hoyle, C. K.; Ward, A. *Biochem. Soc. Trans.* **2000**, *28*, 513−517. (b) Ward, A.; Hoyle, C. J.; Palmer, S. E.; Morrison, S. J.; Langton, K.; O'Reilly, J.; Rutherford, N. G.; Griffith, J. K.; Pos, K. M.; Poolman, B.; Gwynne, M.; Badman, G.; Herbert, R. B.; Henderson, P. J. F. In *Microbial Multidrug Efflux*; Horizon Scientific Press: Wymondham, U.K., 2002; Chapt. 9, pp 121−139, and unpublished data.
(30) Patching, S. G.; Middleton, D. A.; Henderson, P. J. F.; Herbert, R. B. *Org. Biomol. Chem.* **203**, *1*, 2057−2062.
(31) Boland, M. P.; Middleton, D. A. *Magn. Reson. Chem.* **2004**, *42*, 204−211.